Mid-infrared resonant ablation of PMMA

Sanjeev NAITHANI[1], Arnaud GRISARD[2], David SCHAUBROECK[1], Eric LALLIER[2], Geert Van STEENBERGE[1]

[1]Centre for Microsystems Technology (CMST), imec and Ghent University, Technologiepark 914, 9052 Gent, Belgium.
[2]Thales Research & Technology (TRT), Av. Augustin Fresnel 1, 91767 Palaiseau cedex, France.
E-mail: sanjeev.naithani@ugent.be

Nowadays, laser ablation proved to be a reliable micro-fabrication technique for patterning and structuring of both thin film and bulk polymer materials. In most of the industrial cases, ultra-violet (UV) laser sources are employed. Mid-infrared resonant laser ablation (RIA) is a promising and alternative approach, using short pulse mid-infrared laser, which can be wavelength tuned to one of the molecular vibrational transitions of the polymer to be ablated. As a result, the technique is selective in respect of processing a diversity of polymers, which usually have different infrared absorption bands.

In this paper, we present mid-infrared resonant ablation of PMMA (Poly (Methyl MethAcrylate)), employing nanosecond laser pulses tunable between 3 and 4 microns. This RIA laser set-up is based on a commercial laser at 1064 nm wavelength, pumping with ~15 nanosecond pulses a singly resonant Optical Parametric Oscillator (OPO) built around a Periodically-Poled Lithium Niobate (PPLN) crystal with several different Quasi-Phase Matching (QPM) periods. RIA has been successfully demonstrated for structuring bulk PMMA, and selective thin film patterning of PMMA on glass has been implemented.

Keywords: laser machining, mid-infrared laser, PMMA, resonant ablation, tunable laser.

1. Introduction

Several thousand journal publications are devoted to polymer laser ablation, driven by interest in the basic science as well as by numerous applications that have emerged for this high-resolution technique for material removal. The direct-write and contactless nature of the process and the fact that it can be employed under atmospheric conditions and at room temperature, make laser ablation very attractive as micromachining technology.

As most materials absorb very well in the UV and as shorter wavelengths correspond to a better optical resolution of the beam delivery system, UV excimer lasers are very suitable for patterning with micron and even submicron resolution. This is in particular the case when the machined substrate is a polymer since this material features a low thermal conductivity, extremely high UV absorption, and the ability to decompose photo-chemically. During this photochemical ablation process, the incident photons have sufficiently high energy to directly break main chain bonds, restricting the temperature rise, and the extent of thermal damage to the substrate [1].

That a purely thermal process can produce effective polymer ablation has been confirmed by a number of investigations using long wavelength CO_2 lasers, in which the photons couple to vibrational modes of the molecule [2].

A promising approach named resonant infrared laser ablation (RIA) was introduced at the beginning of the 21st century. This method uses a short pulse mid-infrared laser system, which can be wavelength tuned to one of the molecular vibrational transitions of the polymer to be ablated. As a result, the technique is selective in respect of processing a diversity of polymers, which usually have different infrared absorption bands. So far most studies have been carried out using a free electron laser (FEL), providing picosecond pulses tunable between 2 and 10 microns [3]. However, in most applications, FELs are not practical since they are coupled to huge and expensive accelerators. Therefore, new technologies are being developed to replace FELs with bench-top solid-state photonic sources [4] [5]. Most of the resonant infra-red ablation (RIA) studies have been focused on matrix-assisted laser desorption/ ionization mass spectroscopy [6]. However, the utilization of RIA technique in the patterning of thin films has not been explored.

In this paper, we present mid-infrared resonant ablation of PMMA (Poly (Methyl MethAcrylate)) employing nanosecond laser pulses tunable between 3 and 4 microns. The experimental set-up is based on a commercial laser at 1064 nm pumping with ~15 nanosecond pulses at a 20 kHz repetition rate a singly resonant Optical Parametric Oscillator (OPO) built around a Periodically-Poled Lithium Niobate (PPLN) crystal with several Quasi-Phase Matching (QPM) periods, delivering more than 0.3 W of mid-IR power, corresponding to 15 µJ pulses. Moreover, mid-IR resonant ablation has been successfully implemented for patterning thin films of PMMA on a glass substrate, which provides a glimpse of using this technique for patterning applications, where selective removal is very crucial [7].

2. Experimental work

2.1 Sample preparation

Bulk sheets and thin films of PMMA were prepared for resonant and non-resonant mid-infrared ablation experiments. First, bulk sheets of PMMA (Good fellow, PMMA Acrylic sheet, 750 µm) were used for RIA. Next, in order to investigate selective laser patterning of thin films, samples with thicknesses of 650 nm and 1300 nm were prepared. For this application, a specific PMMA solution in anisole (950 PMMA A resist)) was purchased from MICROCHEM technology (Germany). The thin films were obtained by spin coating on a glass substrate (2 inch x 2 inch). Anisole (Bp 154°C) has been removed by evapora-

tion at high temperature (180°C, 90s) on a hot plate immediately after spin coating.

2.2 Infrared spectral analysis

The infrared (IR) absorption spectra of the used PMMA materials were obtained by ATR-IR (Attenuated Total Reflection InfraRed) spectroscopy, using a Bio-Rad 575c FT-IR spectrometer equipped with a golden gate module. The spectrum consists of 32 scans with a resolution of 4 cm^{-1}.

2.3 Mid-infrared ablation set-up

The experimental mid-IR laser set-up as schematically shown in Figure 1, is based on a commercial laser at 1064 nm pumping with ~15 nanosecond pulses at a 20 kHz repetition rate, a singly resonant Optical Parametric Oscillator (OPO) built around a PPLN crystal with several Quasi-Phase Matching (QPM) periods.

In the OPO cavity, the signal can oscillate between 1500 nm to 1650 nm, corresponding to idler wavelengths from 3660 nm to 3000 nm. Coarse tuning can be obtained by translating the PPLN crystal, thus changing the QPM period. Wavelength fine tuning is achieved by heating the crystal, which allows us to achieve a continuous wavelength tuning between 3000 nm and 3600 nm, by combining coarse and fine wavelength tuning.

Taking into account the various filters used after the OPO cavity to remove the remaining pump and signal photons, this OPO delivers more than 0.3 W of mid-IR power, corresponding to 15 µJ pulses.

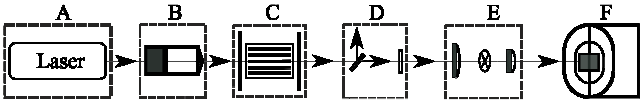

Fig. 1 Schematic diagram of the mid-IR ablation set-up consisting of six sub-divisions: (A) pump laser (B) attenuator / isolator (C) OPO / wavelength conversion unit (D) filtering section (E) beam delivery unit (F) motorized sample stage.

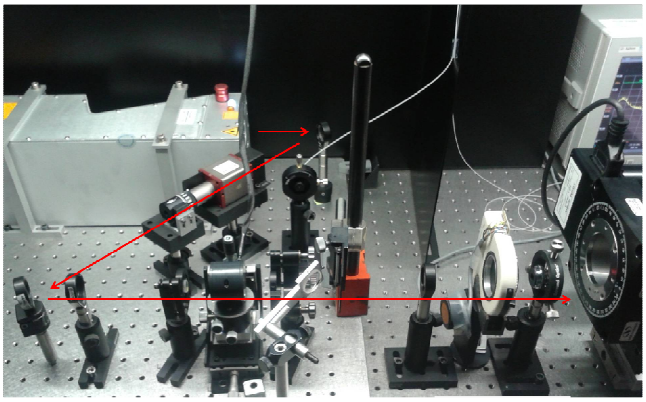

Fig. 2 Photograph of the bench-top mid-IR tunable high power ablation set-up (schematic is illustrated in Figure 1).

The photograph of bench-top mid-IR laser ablation set-up used in these experiments is shown in Figure 2, in which the beam path is depicted by an arrow. The signal wavelength is projected to a free-space-fiber coupler, which is eventually connected to OSA (Optical Spectrum Analyzer). The signal wavelength is measured using an OSA and the corresponding idler wavelength is calculated. In the ablation set-up, the laser beam was focused on the target sample by a beam delivery system consisting of IR microscopic objective (Edmund Optics, 3.75 µm CWL, 6 mm FL ZnSe). The samples were mounted on a motorized rotational stage, allowing a controlled amount of laser shots per spot.

The ablation experiments for the bulk PMMA sheets were conducted for two non-resonant wavelengths (3.20 µm, 3.34 µm) and one resonant (3.39 µm) wavelength. In case of PMMA thin film patterning on glass, the resonant (3.39 µm) wavelength was selected. A pulse repetition rate of 20 kHz, 165 mW output power, with different ablation speeds of 1 to 50 mm/s were used during these experiments.

2.4 Depth profiles

The ablated craters were inspected with an optical microscope. The crater depths were measured with a non-contact optical profiler (Wyko NT3300) and a mechanical profiler (Dektak 150).

2.5 Scanning electron microscopy

Scanning electron microscope (SEM) analysis was performed on a JEOL JSM-5600. The apparatus was used in the secondary electron mode. Prior to analysis, all samples were coated with a thin gold layer (20 nm) via plasma magnetron sputter coating.

3. Results and discussions

A detailed mid-IR absorption spectrum of PMMA obtained by ATR-IR spectroscopy is illustrated in Figure 3.

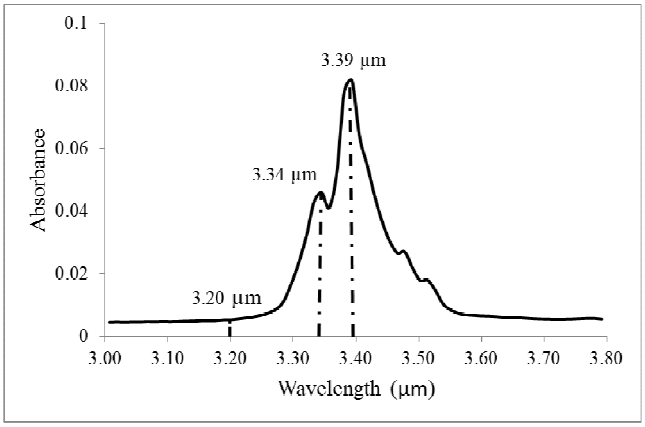

Fig. 3 Mid-infrared absorption spectrum of PMMA indicating a highest peak of absorption at 3.39 µm, a lower peak at 3.34 µm and minimum absorption at 3.20 µm.

It is observed from this figure that there is a maximum peak of absorption at wavelength 3.39 µm which corresponds to the C-H asymmetric stretch in CH_3. Next, a medium peak at 3.34 µm (C-H asymmetric stretch in CH_2) is also noticed. Given the tunability of the laser, we are able to address both peaks, as well as a wavelength of 3.20

which corresponds to minimum absorption in this specific mid-IR range of PMMA.

Experiments on bulk PMMA sheets at the above mentioned resonant and non-resonant absorption wavelengths were performed with various amounts of laser shots. A comparative and qualitative study at three wavelengths has been carried out keeping all other laser parameters (fluence, pulse energy, focusing conditions) fixed.

The quality of the grooves obtained after mid-IR experiments at different wavelengths are shown in Figure 4. On the left, the optical microscopic images are depicted while on the right corresponding SEM micrographs are shown. After ablation at the lowest absorption wavelength (3.20 µm) it is observed that the rim width is more pronounced and the ablated crater depth is shallow (See Fig. 4 (a), (b)). As the wavelength is tuned to the medium absorption wavelength (3.34 µm), the width and depth of the ablated crater increases (Fig. 4 (c), (d)). Interestingly, few tiny particles in the ablated region are present which are attributed to trapped air bubbles during the re-solidification of the material from the molten state. Finally, at the resonant wavelength (3.39 µm), it can be clearly noticed (Fig. 4 (e), (f)) that the ablated grooves width increases further. Moreover, the region is free of debris and / or re-deposited particles.

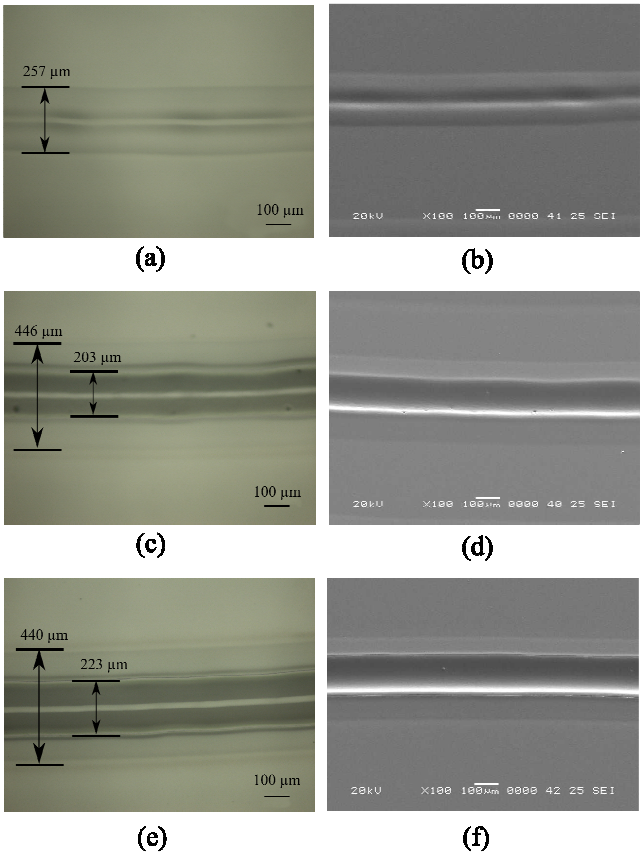

Fig. 4 Mid-IR ablation of PMMA at three wavelengths of operation: 3.20 µm (a), (b); 3.34 µm (c), (d) and 3.39 µm (e), (f). On the left: Optical microscopic images are shown and on the right: Corresponding SEM micrographs are illustrated.

By plotting the ablation depth versus translation speed, or amount of pulses, the ablation behavior of PMMA can be quantified. Results are summarized in Figure 5 and Figure 6 at these three different ablation wavelengths. Indeed, as expected, the influence of the wavelength on ablation is significant.

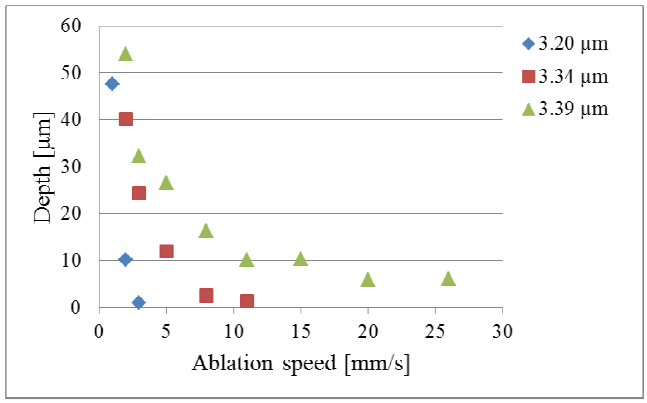

Fig. 5 Ablation depth plots of PMMA at three different wavelengths: 3.20 µm, 3.34 µm and 3.39 µm.

Now, if we compare the slopes in Figure 6, the influence of the laser wavelength on the ablation rate (amount of material removed per laser pulse), which varies from 54 nm per laser pulse for non-resonant ablation to 77 nm per laser pulse for resonant ablation. Furthermore, the influence of laser wavelength on the incubation effect is pronounced. In general, incubation occurs when a weakly absorbing polymer material is converted to a material with a higher absorption cross-section after repetitive exposure through photo-chemical and/or photo-thermal reactions.

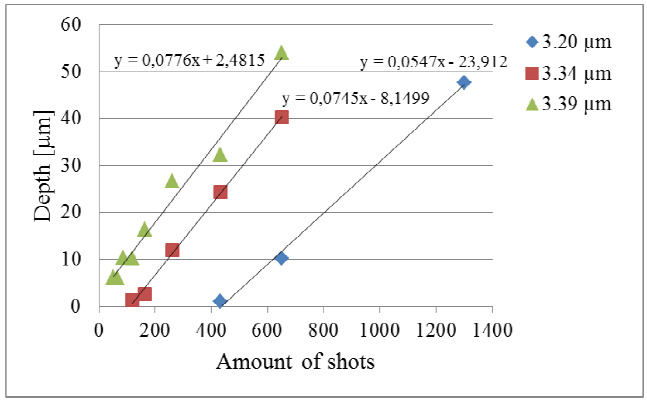

Fig. 6 Ablation rate plots for PMMA at three different mid-IR wavelengths of absorption: 3.20 µm, 3.34 µm and 3.39µm.

Whereas for resonant ablation incubation is limited, which is different for non-resonant ablation, where we need more than 400 laser pulses before material removal occurs. From Figure 6, with 400 shots per location the ablation depth at 3.20 µm wavelength is almost negligible. At 3.34 µm and 3.39 µm, the depths were much higher: 24 µm and 32 µm, respectively.

This behavior of incubation and given tunability of RIA source can be exploited in case of selective laser patterning of a polymer on another polymer. For selective ablation, it

is very important to remove the top layer without damaging the underneath layer (Figure 7).

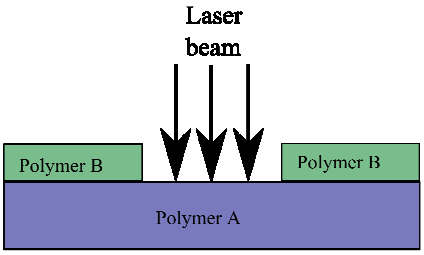

Fig. 7 Schematic diagram for selective ablation process of a polymer (Polymer B) on another polymer (Polymer A).

For the patterning applications, experiments were conducted at 20 kHz, 165 mW and output wavelength was tuned to the resonant peak (3.39 µm) of absorption. In this case, the laser fluence has been maximized by using a mid-IR microscopic objective (focal length 6 mm). The laser spot size was not measured exactly, but estimated from crater depth profile as indicated in Figure 8. The calculated fluence for thin films patterning with this mid-IR ablation set-up and estimated spot size of 17.1 µm (Full Width Half Maximum) is approximately 6.5 J /cm^2.

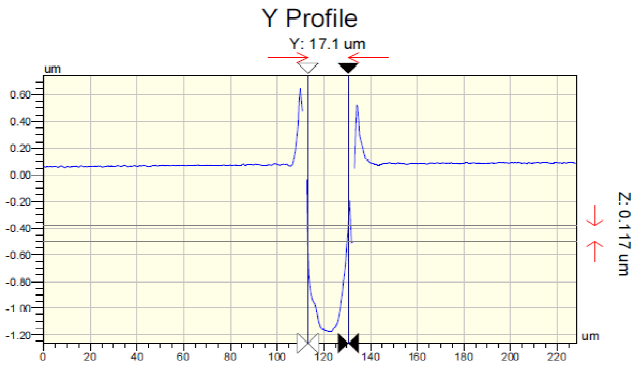

Fig. 8 Cross-section profile of an ablated structure indicating a spot size of 17.1 µm at full-width-half-maximum (FWHM).

The ablation results of PMMA thin films patterning on glass substrate are illustrated in Figure 9. The optical images in Figure 9(a) and Figure 9(b), show clean and debris free ablated tracks with widths of 19 µm and 22 µm (including the rims). Next, the depth profiles shown in Figure 9(b) and Figure 9(d) indicate the removal of about 648 nm and 1298 nm respectively. These values are very close to the initial PMMA thin film thicknesses i.e. 650 nm and 1300 nm.

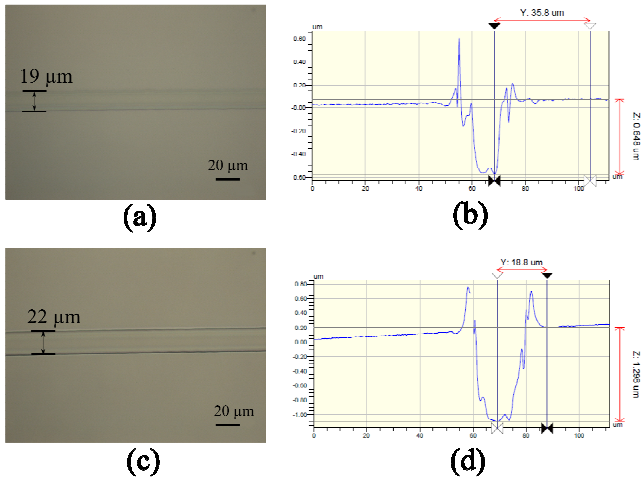

Fig. 9 Optical microscopic images: (a) and (c), of RIA patterned 650 nm and 1300 nm thin films PMMA on a glass. On the right: (b) and (d), are the corresponding depth profiles indicating a removal of 648 nm and 1298 nm of PMMA thin films.

Moreover, the SEM micrographs (Figure 10) of the ablated regions with higher magnification (x1000) are clean and there is no visible re-deposition or debris on the ablated tracks.

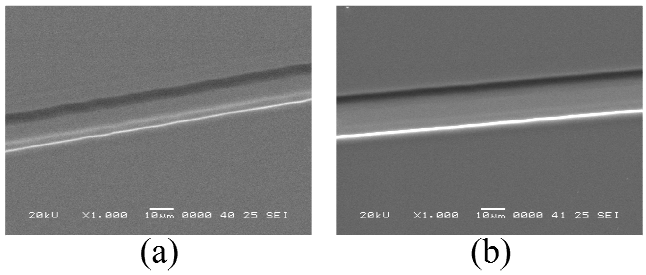

Fig. 10 SEM micrographs of the thin films patterned PMMA (a) 650 nm (b) 1300 nm. The micrographs are taken with 45 degree tilt and 1000 magnification.

It is inferred from these observations that the ablation is likely to be driven by photo-thermal mechanisms. The laser energy deposited into PMMA target is transformed into heat. Resonant infra-red (3.39 µm) excitations of localized molecular-vibrations couple to the phonon within hundreds of fs to ps. This leads to heat accumulation in the material. The thermal energy can be diffused from the localized volume in its thermal confinement time. When the spot size of the laser beam is much larger than absorption length of the material to be ablated, one dimensional thermal diffusion can be assumed. In such a case, the thermal confinement time can be calculated by using the following equation:

$$\tau_{th} = c_p \rho / \alpha^2 K \qquad (1)$$

where τ_{th} is thermal confinement time, c_p is specific heat, ρ is material density, α is the absorption coefficient and K is thermal conductivity. Plugging some numerical values into this formula for PMMA, as c_p ~1466 J / Kg-K, ρ ~1.18 g / cm^3, α ~1730 cm^{-1} and thermal conductivity of PMMA varies from 0.167 to 0.251 W / m-K. This calculation leads to thermal confinement time of ~0.29 ms (for K = 0.200 W / m-K), which is much higher than the laser pulse duration

(~ nanoseconds). Since the time required for the heat to diffuse out of the localized volume is much higher than the laser pulse length, thus this RIA ablation mechanism for PMMA assumed to be photo-thermal in nature.

4. Conclusions

A qualitative and quantitative analysis of the resonant mid-IR laser ablation (RIA) of bulk PMMA has been successfully demonstrated using a recently developed mid-IR tunable source. Higher ablation rates were observed at the resonant wavelength of operation and the ablated crater was free of debris. A proof of concept of thin film PMMA patterning on glass has been provided. Incubation for thin-film patterning using RIA still needs to be investigated in more detail.

5. Acknowledgement

This work was conducted in the framework of the project “IMPROV”, funded within the European Commission FP7 program.

References

[1] R. Srinivasan and W. J. Leigh: J. Am. Chem. Soc., 104(24), (1982) 6784.

[2] J. H. Brannon and J. R. Lankard: Appl. Phys. Lett., 48(18), (1986)1226.

[3] D. M. Bubb, J. S. Horwitz, J. H. Callahan, R. A. McGill, E. J. Houser, D. B. Chrisey, M. R. Papantonakis, R. F. Haglund, Jr., M. C. Galicia and A. Vertes: J. Vac. Sci. Technol., A19(5), (2001) 2698.

[4] The European commission “IMPROV” project: http://www.fp7project-improv.eu (Website as viewed on 16/07/2013).

[5] M. Duering, R. Haglund and B. Luther-Davies: Proc. Optical Society of America, CLEO, QELS, (2010) CMH3.

[6] W. P. Hess, H. K. Park, O. Yavas and R. F. Haglund Jr: Appl. Surf. Sci., 127-129, (1998) 235.

[7] S. Naithani, D. Schaubroeck, Y. Vercammen, R. Mandamparambil, I. Takimets, L. V. Vaeck, G. V. Steenberge: Appl. Surf. Sci., 280, (2013) 504.